

# Liquid Impact Based Material Micro-Forming Technology

V. Samardzic, E.S. Geskin, G.A. Atanov, A.N. Semko, and A. Kovaliov

(Submitted February 7, 2007; in revised form February 23, 2007)

The objective of this study was to investigate material deformation in the course of a high-speed (>1500 m/s) water impact and to use the acquired knowledge for improvement of the forming technology. An experimental setup for projectile fabrication was constructed and a series of experiments involving sub-millimeter and micron scale metal deformation was performed. The geometry and topography of the generated samples were investigated using advanced surface examination techniques and the feasibility of the liquid impact based micro-forming technology was demonstrated.

**Keywords** extrusion, liquid impact, liquid projectile, micro-forming, micro-channel, precision, stamping

## 1. Introduction

The objective of the performed study was to investigate the application of high-speed liquid projectiles for material forming, specifically for formation of submillimeter and micron scale parts. The proposed technology involves impacting a workpiece supported by a die by a high-speed (1000-1750 m/s) water projectile (an impulsive jet) (Ref 1-5). The projectiles are generated by a launcher (a water cannon), which constitutes a modified gun, loaded by a round where a solid slug is replaced by a container with a liquid, e.g., water (Fig. 1). The powder explosion accelerates water and at the end of the barrel the water speed is comparable with that of the solid projectile. The further acceleration occurs in a nozzle attached to the barrel. This enables us to increase significantly the water speed. In the previous experiments, a water velocity of 1750 m/s was achieved. Computations show that it is possible to achieve water speed as high as 3-4 km/s. At the speed of 1500 m/s, the pressure exerted on a target at the impact zone is in an order of 1 GPa. At such a pressure, a metal target impacted by the liquid projectile acquires a shape of the supporting die. Thus, the liquid impact can be used for metal forming and the high-speed liquid projectile can replace a punch.

A water projectile impacting a solid surface at the speed of 1000 m/s and more acts as an explosive, which detonates on the target's surface. Advantages of the impact based forming (Ref 6) as well as the explosive forming (Ref 7-9) are well understood and documented. In a number of applications, however, the use of an explosive is difficult if not impossible.

In this case, the high-speed liquid projectiles can be used as a forming or welding tool. Previous research showed the feasibility of the application of the liquid impact to metal forging, stamping, coining, and extrusion (Ref 10, 11). The most promising application of the liquid projectile, however, is mass production of MEMS parts.

Micro-forming is fabrication of parts or structures with at least two dimensions in the submillimeter range by the use of a forming technology. The effectiveness of the application of the plastic deformation for mass production of micro-parts is quite obvious. It can be the only practical way for mass production of metal and alloy micro-parts. While implementation of the micro-fabrication will revolutionize the MEMS fabrication technology, substantial obstacles are to be overcome in order to achieve this goal. The micro-forming cannot be developed just by scaling down existing forming processes. New techniques must be found for micro-scale deformation of various technological materials at desired rate and accuracy and at an acceptable cost.

Deformation of a target material in the course of a high-speed liquid impact was investigated experimentally. The previous research demonstrated the feasibility of the use of high-speed projectiles as a punch in conventional metal forming operations. The objective of this study is to expand the range of the application of the liquid impact to micro-forming operations. The performed study involved micro- and submillimeter stamping and extrusion of various metals. The performed experiments showed that high-speed liquid projectiles have a potential of becoming a competitive micro-forming tool. Of course a number of issues pertinent to the selection of the energy source for the water acceleration, energy transfer from a source to the projectile, reliability of the launcher and a

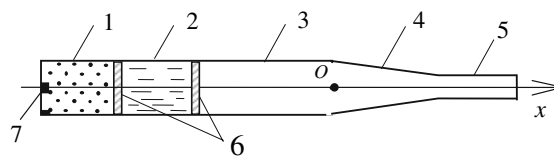


**Fig. 1** Schematic of water cannon. 1—powder charge, 2—water load (projectile), 3—barrel, 4—nozzle, 5—cylindrical attachment (collimator), 6—partitions, 7—primer

This article was presented at Materials Science & Technology 2006, Innovations in Metal Forming symposium held in Cincinnati, OH, October 15-19, 2006.

V. Samardzic and E.S. Geskin, New Jersey Institute of Technology, Newark, NJ; Contact e-mail: vxs9076@njit.edu. G.A. Atanov, A.N. Semko, and A. Kovaliov, Donetsk National University, Donetsk, Ukraine.

guiding system, die design and reliability, etc. must be addressed. However, the feasibility to generate a desired micro-scale deformation of a target material using the liquid impact was demonstrated by the performed experiments.

## 2. Existing Micro-Forming Technologies

Research in micro- and meso-manufacturing area is being conducted by a team lead by Kuniaki Dohda (Ref 12), Gifu University, Japan. Micro-pressing technology has been developed. This technology involved formation of the ultra fine holes in aluminum samples using  $15\ \mu\text{m}$  SiC fibers as a punch. Micro-forging was used to die forge micro-parts out of amorphous alloy. Micro-extrusion of aluminum alloys was investigated as well. A single process system was designed and used for each application (micro-press, micro-extruder). Development of a system which could be used for more than a single micro-forming application and which would have higher efficiency was addressed by a group of Hye-Jin Lee of Korean Institute of Industrial Technology, Korea (Ref 13). Study of forming of the submillimeter metal parts is currently being carried out in the Friedrich-Alexander University, Germany (Ref 14). A Group Mass-micro of Dr. Jiangho Lin, (U of B), is currently working on the development of technologies of mass production of micro-parts (Ref 15). While the teams above are involved in one or another miniaturization of forming facilities, the objective of the proposed study is modification of the mode of the generation of the stress field in a target.

## 3. Experimental Technique

An experimental setup (Fig. 2), for the study of the liquid impact based forming was designed and constructed. In this setup samples to be processed were mounted on a heavy pendulum, which was displaced by the water impact. The angular displacement of pendulum was measured in each experiment and the projectile impulse and momentum were calculated by the use of the measured pendulum displacement. During an experiment, the water cannon was placed at a desired

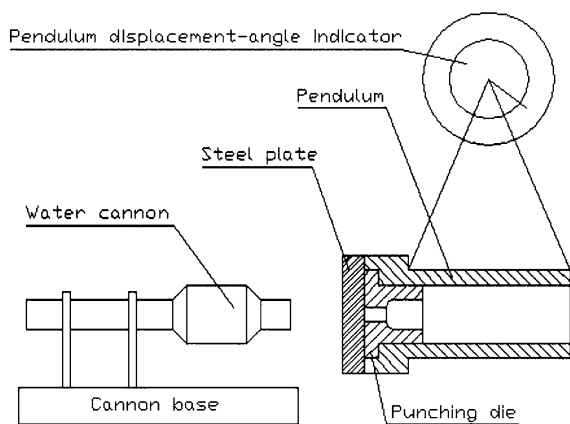


**Fig. 2** Schematic of the experimental setup. Notice that mounting of the target on a ballistic pendulum allows measuring the impact momentum

distance from a sample which then was impacted at selected conditions. In the course of the impact, the target acquired a shape of a supporting die. The principal challenge in the die fabrication was formation of the submillimeter and micron scale cavities using conventional machining facilities (lathe, milling machine, etc.) During each experiment, the values of water mass, powder mass, standoff distance, and pendulum displacement were measured and the acquired data were incorporated into a global matrix of the investigation. On completion of an experiment generated samples were examined visually and then sample characterization, involving scanning electron microscopy, infinite focus microscopy, optical microscopy, 3D digital microscopy, and 3D digital profiler, was carried out.

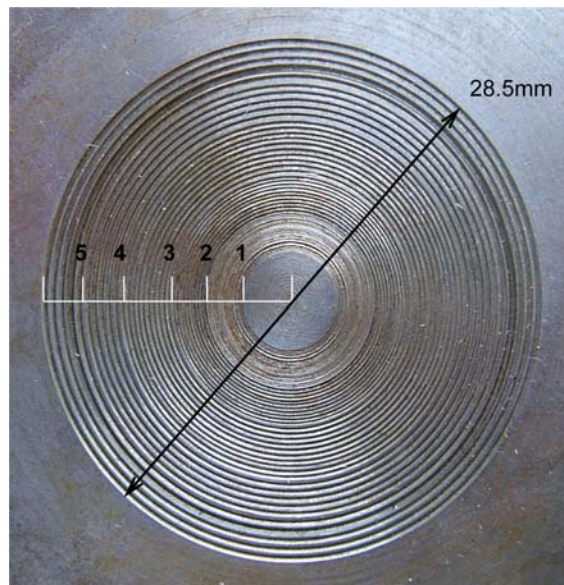


**Fig. 3** General view of the die used for fine forging of samples. Notice complexity of die geometry. Numbers 1–5 show number of the section on the die surface. The ridges geometry of different section (Table 1) is different

**Table 1** Designed parameters of the grooves to be generated on the die surface

Section	1	2	3	4	5
Step, $h$ mm	0.1	0.2	0.3	0.4	0.5
Depth, $b$ mm	0.05	0.1	0.15	0.2	0.25
Number of grooves	20	10	10	5	5

Notice difference in groove geometry at different sections

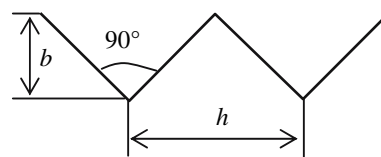


**Fig. 4** Desired geometry of the ridges

The fabricated dies enabled us to examine various micro-forming technologies. Both, the submillimeter and micron scale deformations were investigated. The study involved filling cavities by a target material and stamping a die shape on the target surface. The filling of the semi-closed cavities (groves on the workpiece surface) and metal extrusion into open micron scale slots was examined. Stamping using simple (cylindrical wires) and complex (a coin) dies was also investigated. Targets

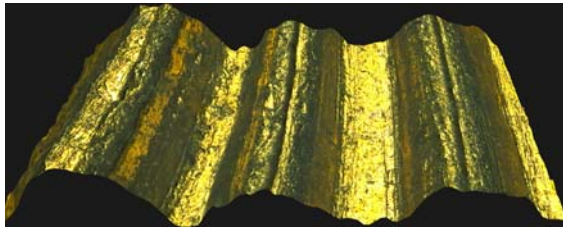


**Fig. 5** Segment of concentric grooves and ridges formed on brass. Notice that ridges and grooves of the workpiece surface have the forms of a trapezium, which is similar to a corresponding segment of the die

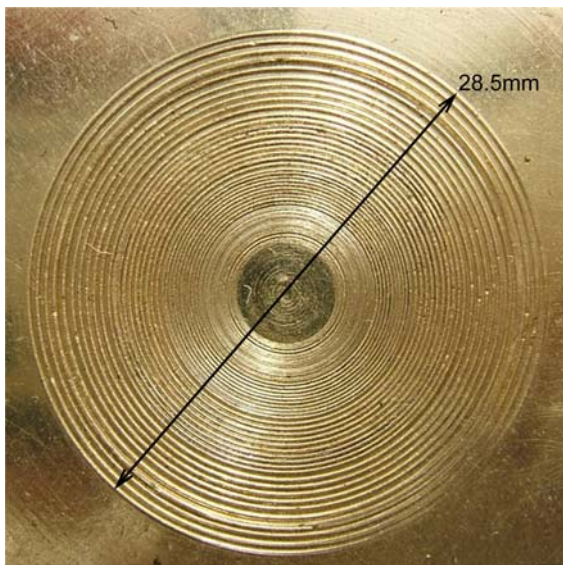


**Fig. 6** General view of concentric grooves and ridges formed on the surface of brass sample. Notice precise geometry of the generated grooves

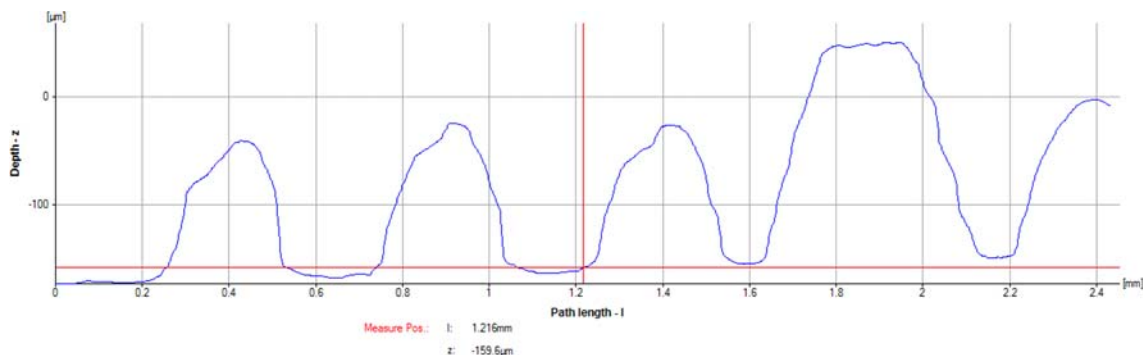


**Fig. 7** The profile of concentric grooves and ridges formed on a brass sample

were fabricated from copper, brass, aluminum, and steel. In one of the performed experiments, extrusion of an alloy used for fabrication of Ukrainian coins was studied.

An exit diameter of the nozzle used in the performed experiments was 15 mm, the diameter of barrel was 20 mm and the total length of the launcher was 80 cm. Amount of water used for the projectile formation ranged between 30 and 350 g. Water was propelled by the products of the combustion of 30 g powder. The standoff distance was 16 cm in all experiments. Calculated outflow velocity of the projectile head ranged between 850 and 1566 m/s. Calculated maximal pressure inside the nozzle ranged from 341 and 843 MPa. At these conditions, the pressure exerted on the workpiece varied from 0.35 to 1.2 GPa.

## 4. Details of an Experimental Procedure and Results

### 4.1 Formation of Submillimeter Scale Grooves

The experiments involved the study of formation of submillimeter circumferential ridges on the target surface. For this study, a die with concentric groves was designed and manufactured. The general view of the die surface is depicted in Fig. 3. The design parameters of the die groves are given in Table 1 and Fig. 4, which shows desired geometry of cross section of two adjacent groves. Here  $b$  stands for the depth of the groove on the die surface and  $h$  is the pitch of the grooves. In order to investigate the effect of the groove geometry on the result of forming five distinct sets of the grooves were generated on the die surface. Correspondingly the die surface was divided into five sections. The actual shape of the die differed from the designed geometry. This difference was due to slipping of cutting tool and vibrations of tool and work piece in the course of turning. While the designed groves had a triangular profile, due to the limitations of the machining facility used for die manufacturing the grooves and ridges generated on the die surface had a shape of a trapezium. It should be noted that the accuracy of machining of the die surface changes across the die radius. The accuracy of Sections 3-5 was adequate while the larger deviations from desired geometry were found within Sections 1 and 2.

In the course of experiments, a metal plate was placed on the die and impacted by a projectile. The impact forced the target material to fill the die grooves thus a set of ridges and groves was formed on the target surfaces. Compliance between the

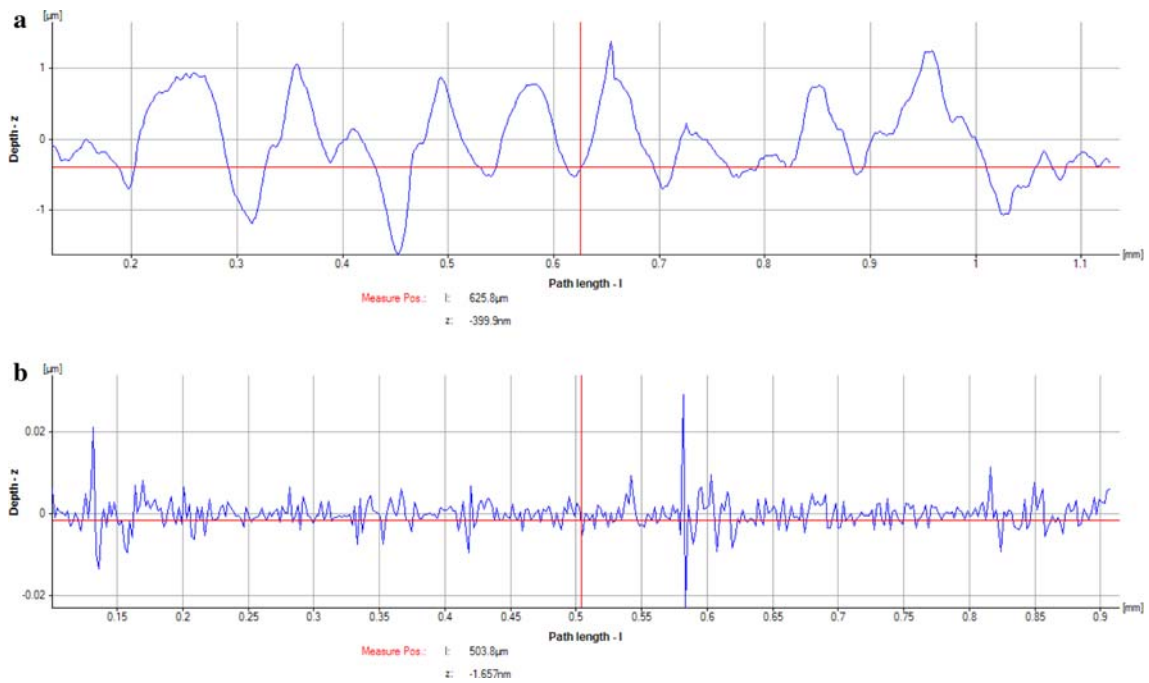


**Fig. 8** (a) Surface waviness of grooves formed on a brass sample, (b) surface roughness of grooves formed on a brass sample

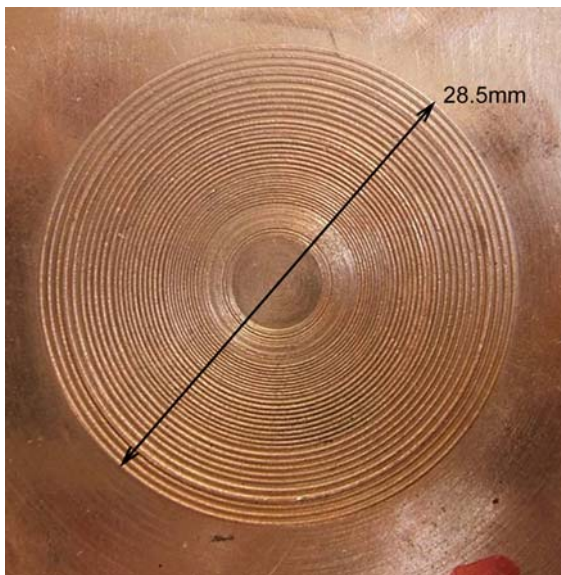


**Fig. 9** General view of concentric grooves and ridges formed on the surface of a copper sample

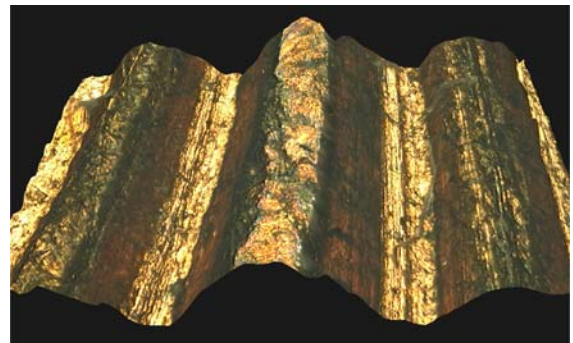


**Fig. 10** Segment of concentric grooves and ridges formed on a copper sample

geometries of the die and workpiece surfaces as well as the topography of the generated surface constituted the criterion of the quality of the performed forming operation. The performed study was carried out at the following experimental conditions: 200 g of water propelled by 30 g of gun powder at a stand of distance of 16 cm. At these conditions, a computed projectiles impact velocity was 1500 m/s and a period of pendulum oscillation was 2.35 s.

In order to quantify the accuracy of forming the microscopic evaluation of a workpiece was carried out using the optical microscopy, 3D digital microscopy, and infinite focus microscopy. The optical microscopy (200 $\times$ ) was used for visual

examination of the generated surfaces. The performed examination confirmed that at the existing tolerances of die fabrication there is sufficient compliance between the desired die geometry and the actual geometry of a workpiece.

The surface geometry generated in the course of an impact of a brass sample is shown in Fig. 5-8. Close up view of segment containing three ridges reproduced by 3D digital microscopy also confirms compliance of the shapes of the die and the workpiece (Fig. 5). Formed shape is a mirror view of the corresponding die section. Similar result was obtained for 10 different sections of the workpiece surface.

A general view of the surface of a brass target generated in the course of forming is shown in Fig. 6. As it follows from this figure, the micro-scale geometries of the die and the workpiece complied sufficiently well and the geometries of the grooves and ridges on both surfaces are almost identical. This accurate reproduction of the die geometry was observed in all sections.

An infinite focus microscopy was used for quantification of the workpiece surface topography. Profiles of four neighboring ridges formed on the brass surface are shown in Fig. 7, where

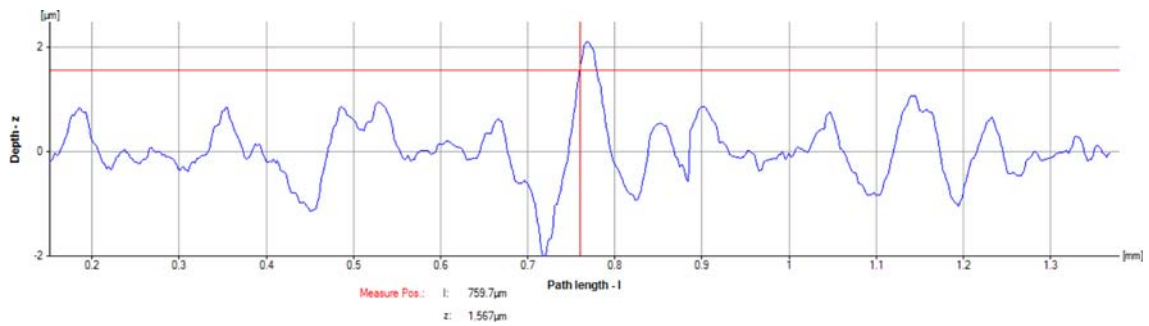


**Fig. 11** Surface waviness of groves formed on a copper sample

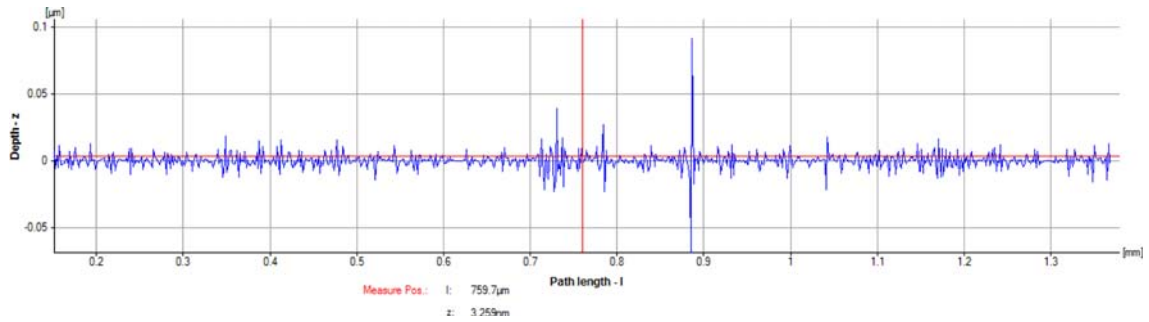


**Fig. 12** Surface roughness of a groove formed on a copper sample



**Fig. 13** General view of a coin stamped on aluminum and copper samples. Notice reproduction of fine details of the coin on the sample surface

three ridges have height of approximately  $140\ \mu\text{m}$  while neighboring ridge has height of approximately  $200\ \mu\text{m}$ . The difference in size of these ridges was the same as that of the corresponding parts of the die and was caused by an unstable process of the die machining.

Investigation of other segments of the workpiece surface by infinite focus microscopy produced similar results. This method was also used for analysis of the surface waviness and roughness of all generated samples. As it follows from Fig. 8(a) and (b), the surface waviness was below  $2\ \mu\text{m}$  and the roughness was below  $0.04\ \mu\text{m}$ .

A general view of formed groves and ridges on the surface of copper sample is shown in Fig. 9. Notice that the desired

surface geometry was accurately reproduced in the course of the impact. This compliance is also demonstrated by a close up view of a segment containing three ridges and reproduced by 3D digital microscopy (Fig. 10).

The infinite focus microscopy was used to examine the topography and profile of a copper sample. It was found that the waviness of the generated surface was below  $2\ \mu\text{m}$  (Fig. 11) and roughness was below  $0.1\ \mu\text{m}$  (Fig. 12).

#### **4.2 Fine Stamping**

The objective of these experiments was the study of formation of rather complex patterns on the target surface. In

this case, a conventional coin was used as a supporting die. Target materials included copper, brass, aluminum, and high ductility steel. The steel had 46% elongation, tensile strength of 325 MPa, and yield strength of 195 MPa. Thickness of the copper and brass samples was 3 mm and steel samples were 2.5 mm thick.

An Ukrainian coin was used as a die for investigation of the fine stamping. As a result the coin image was stamped into copper, steel, and aluminum plates. In the course of the experiments, 350 g of water were propelled by combustion of 35 g of gun powder at a stand off distance of 16 cm. A calculated impact velocity was 850 m/s. Geometry of the coin

was accurately reproduced on all samples, aluminum, steel, and copper. Quality of reproduced surface was characterized by two methods, infinite focus microscopy and 3D profile analysis. Measurement of parameters of the surface geometry was performed and it was demonstrated that the coin geometry was reproduced sufficiently accurate on the surface of all targets.

General view of the coin images stamped on the surface of aluminum and copper samples is shown in Fig. 13. An image of the coin stamped on the surface of a steel sample and generated by the 3D profile analysis is shown in Fig. 14. The depth of the depression of the workpiece surface was approximately 130  $\mu\text{m}$ . As it was demonstrated by measurements, this corresponds to the topography of the coin. In addition to the profile and depth features, top view of the workpiece geometry

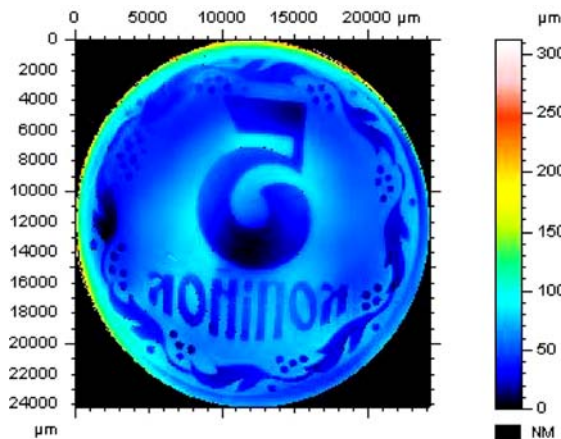


**Fig. 14** Image of coin stamped on steel created using 3D profile analyzer

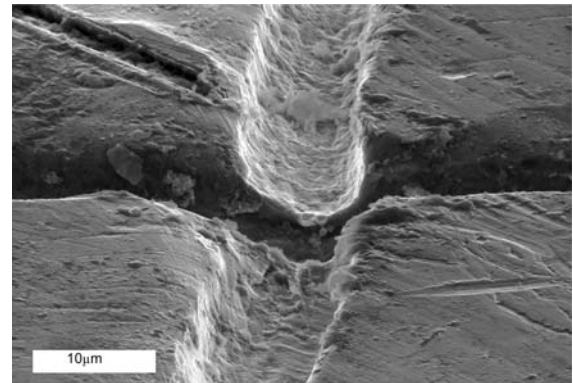


**Fig. 17** Intersection of two micro-channels formed on the brass surface by 7  $\mu\text{m}$  diameter tungsten wire

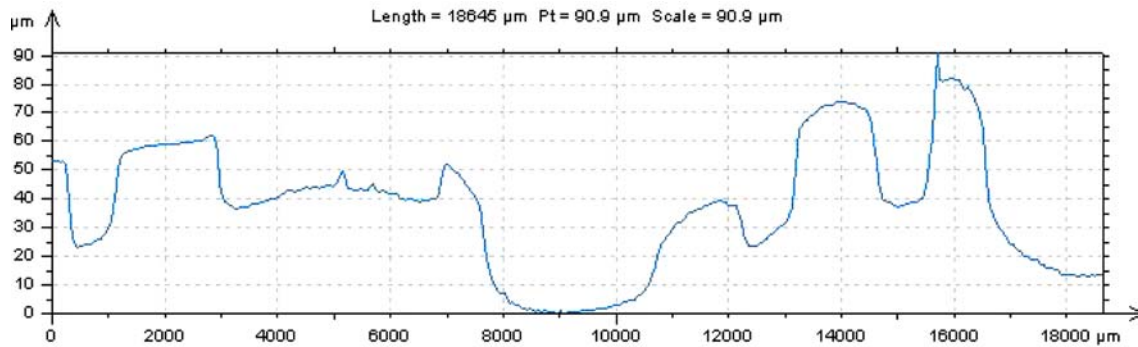


**Fig. 15** Example of profile of a coin stamped on a steel sample

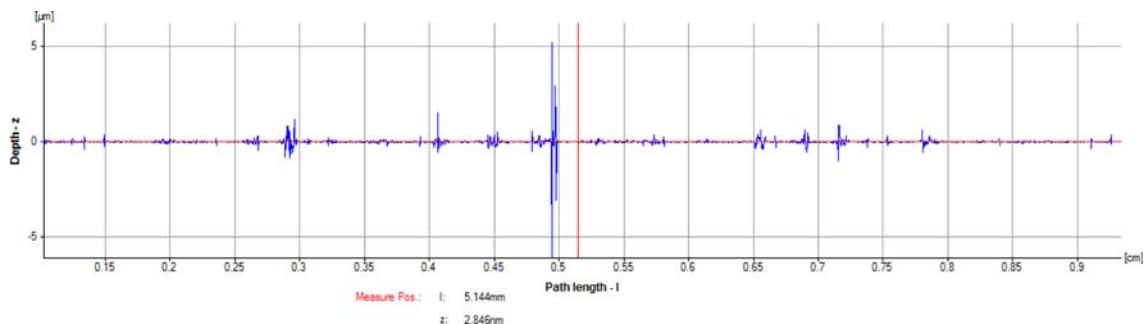


**Fig. 16** Roughness of the surface of steel sample stamped by a coin

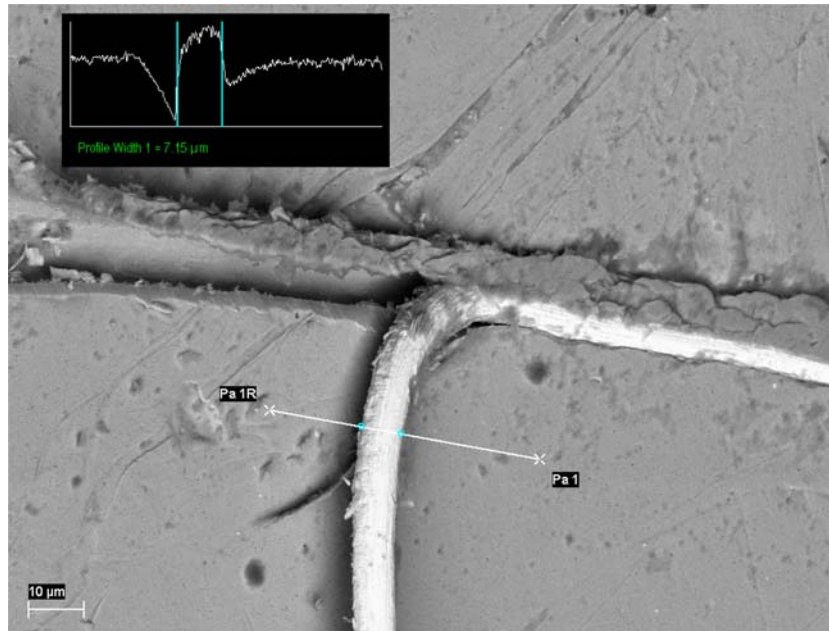


**Fig. 18** A view of the 7  $\mu\text{m}$  tungsten wire embedded into brass surface generated by SEM

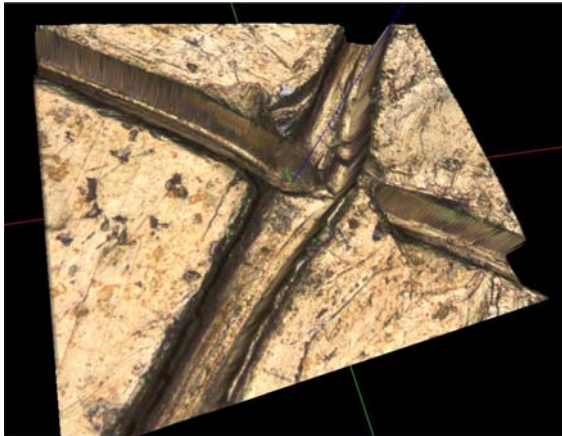


**Fig. 19** Intersection of two micro-channels formed on a brass sample by 40  $\mu\text{m}$  diameter tungsten wires

was compared to the corresponding view of the die. The performed measurements showed almost mirror like reproduction of the die geometry on the workpiece surface. Example of a profile of the coin (Fig. 15) shows fine stamped features with the maximum height range of 90  $\mu\text{m}$  and the roughness below 1  $\mu\text{m}$  (Fig. 16).

### 4.3 Microns Scale Forming

The objective of the performed experiments was to form micro-channels on the surface of different metals. During the tests individual micro-channels and micro-channel's networks were formed on the surface of cooper, brass, and steel samples. High-ductility steel having 46% elongation, tensile strength of 325 MPa, and yield strength of 195 MPa was used in this study. A tungsten wire was used as a die. The wire diameters were 7 and 40  $\mu\text{m}$ . In each experiment, the wire was attached by glue to a polished surface of a metal sample in order to form

a desired network. Samples were mounted on a heavy pendulum with the wire side facing the pendulum. Water projectiles impacted opposite side of the sample and as a result much harder wires were driven into softer materials of samples creating a desired network of micro-channels. In the course of experiments, 230 g of water were propelled by 30 g of a gun powder at a standoff distance of 16 cm.

Geometry of the generated micro-channels was examined by optical microscopy, infinite focus microscopy, scanning electron microscopy, 3D digital microscope, and surface profiler. Scanning electron microscope was used to investigate surfaces of formed micro-channels. Intersection of two micro-channels formed by 7  $\mu\text{m}$  diameter tungsten wire on brass sample is depicted in Fig. 17. Examination showed that formed channels are approximately 8  $\mu\text{m}$  wide. A view and dimensions of 7  $\mu\text{m}$  diameter tungsten wire embedded into brass sample are shown in Fig. 18.

Infinite focus microscopy was used to perform topography, profile, waviness, and roughness analyses. Intersection of two micro-channels formed on brass by 40  $\mu\text{m}$  diameter tungsten wire is shown in Fig. 19.

Three-dimensional microscope was also used for examination of the formed micro-channels (Fig. 20 and 21). Generated 3D images of channels were further used for profile analysis and the results complied with previously conducted infinite focus microscopy analysis. A 3D image of a section of the micro-channel formed on the brass sample by 40  $\mu\text{m}$  diameter tungsten wire is shown in Fig. 20 and a 3D image of an intersection of micro-channels formed on the brass sample by 40  $\mu\text{m}$  diameter tungsten wire is shown in Fig. 21. Extensive examination of formed micro-channels confirmed geometrical reproducibility and the exceptional surface quality.

Profile analysis performed by the infinite focus microscopy revealed steady geometry of the formed channels. An example of the channel profile (Fig. 22) indicates that both the depth and the width of formed channels are approximately 40  $\mu\text{m}$ . Curvature of the 7  $\mu\text{m}$  wire has better

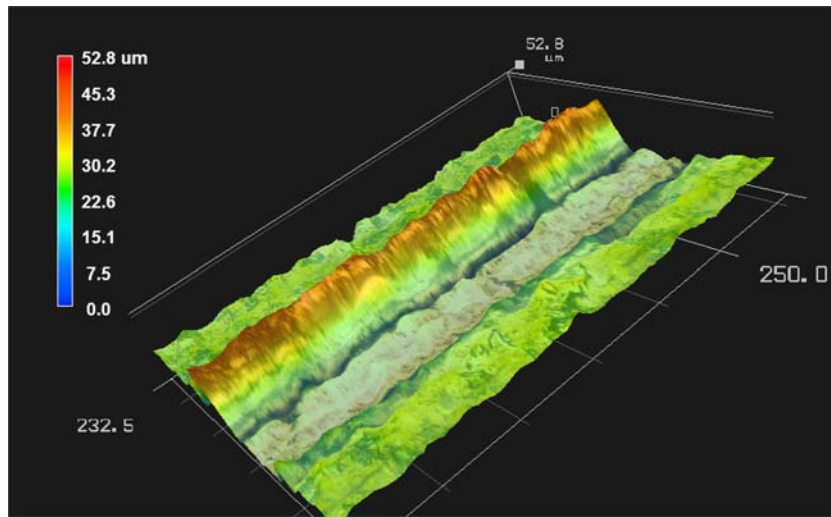


**Fig. 20** A 3D image of a section of the micro-channel formed on a brass surface by 40  $\mu\text{m}$  diameter tungsten wire; the image is generated by the 3D digital microscope

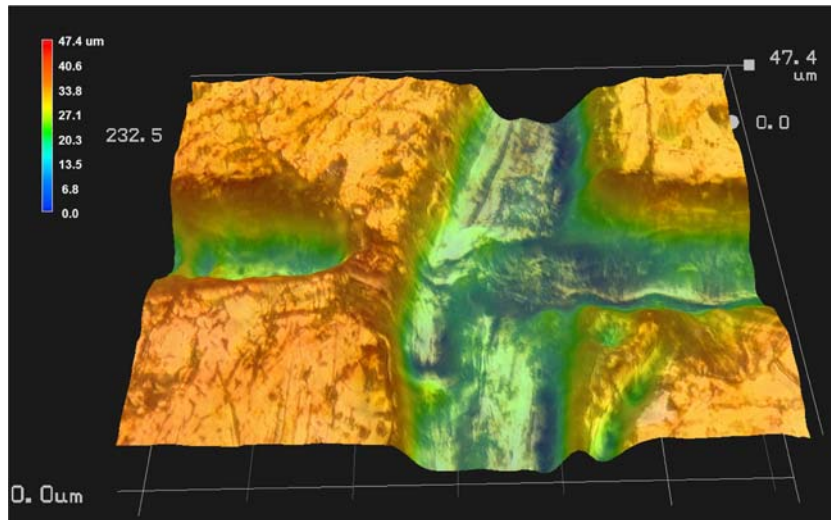


**Fig. 21** A 3D image of an intersection of the micro-channels formed on a brass surface by 40  $\mu\text{m}$  diameter tungsten wire; the image is generated by the 3D digital microscope

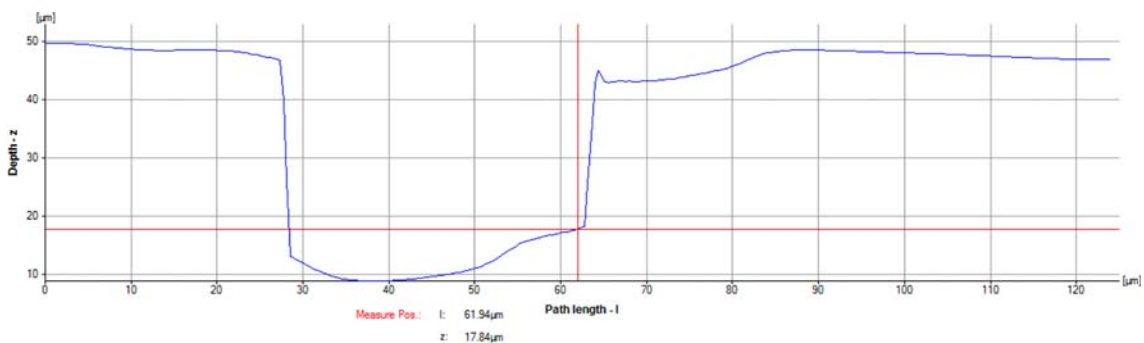


**Fig. 22** A profile of the channel formed on a brass sample by the 40  $\mu\text{m}$  wire. Notice that the depth and width of the channel are approximately equal to the wire diameter

imprint on all of tested materials. This is demonstrated by two profiles, which have depth and width in the range of wire diameter. At the same time, the curvature of the

generated channel is completely determined by the geometry of the wire (Fig. 23). Profile of same section of the channel is also shown in Fig. 24.



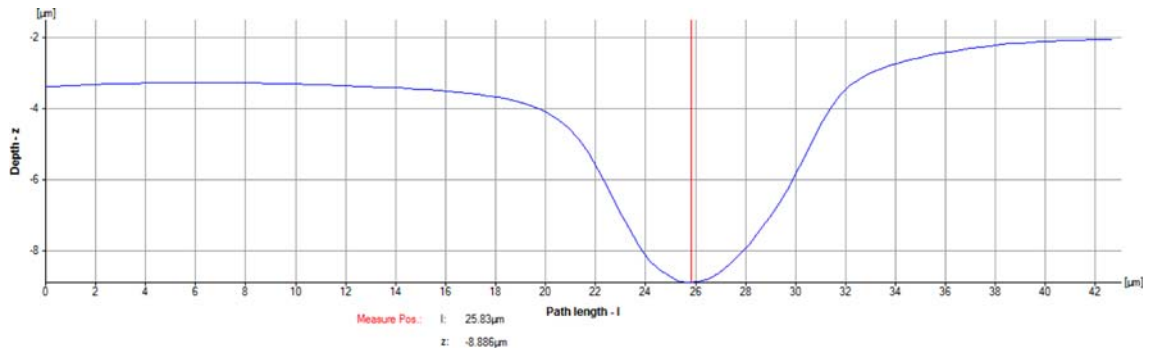


**Fig. 23** Profile of the channel formed by a 7 μm diameter wire. Notice the compliance between profile of the channel and the die

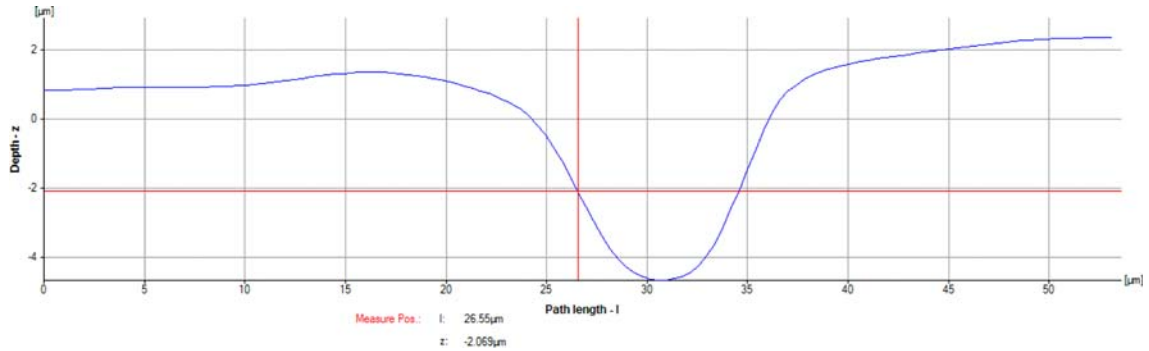


**Fig. 24** Profile of the channel formed by 7 μm diameter wire. Notice the compliance between profile of the channel and the die and almost identity of profiles Fig. 23 and 24

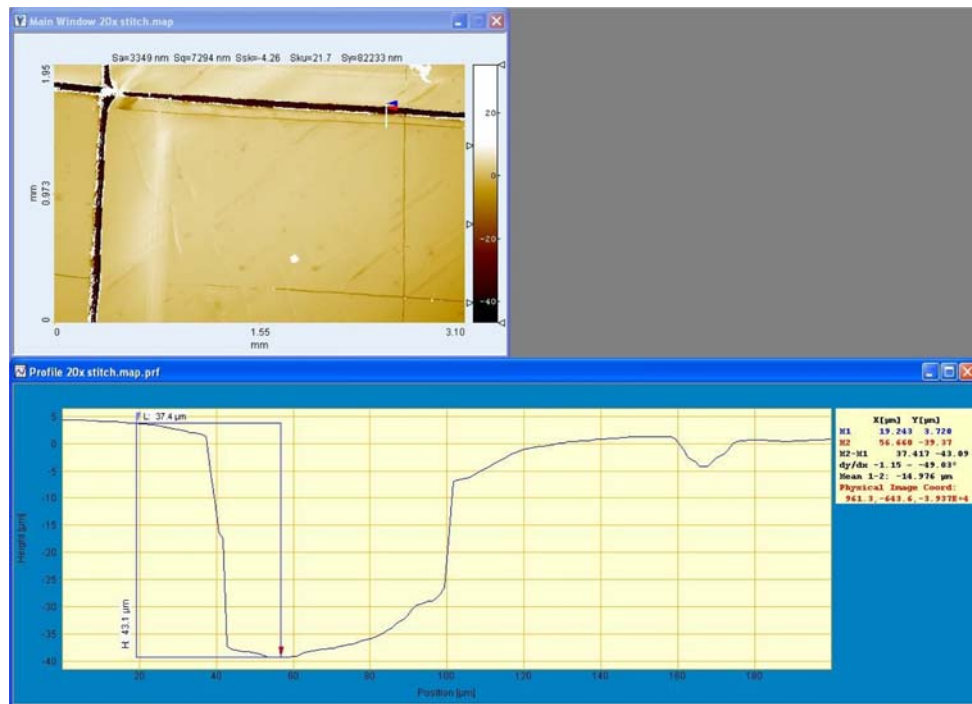


**Fig. 25** Profiles of two adjacent channels 40 and 7 μm wide

Additional analysis of the profile and roughness of channels was conducted by a table version of the white light non-contact 3D optical profiler. This instrument was used to scan surfaces

with embedded micro-channels. This analysis yielded results compatible to those obtained by the infinite focus microscopy. This confirmed consistency of the forming.

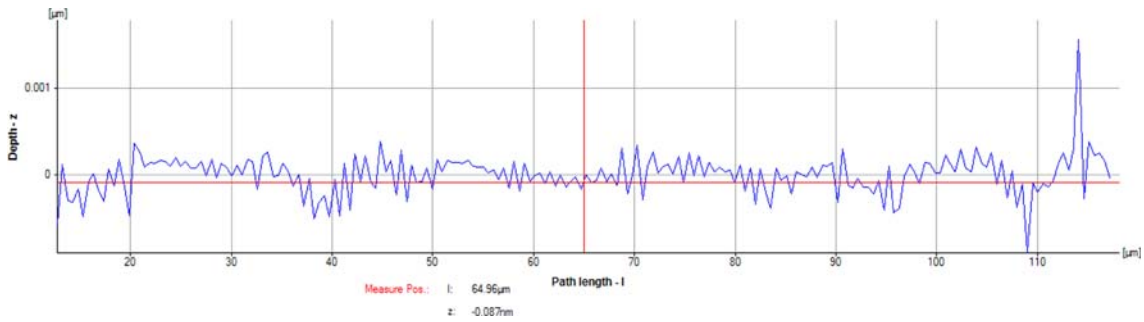


**Fig. 26** Surface roughness of a channel formed by the 40  $\mu\text{m}$  wide wire

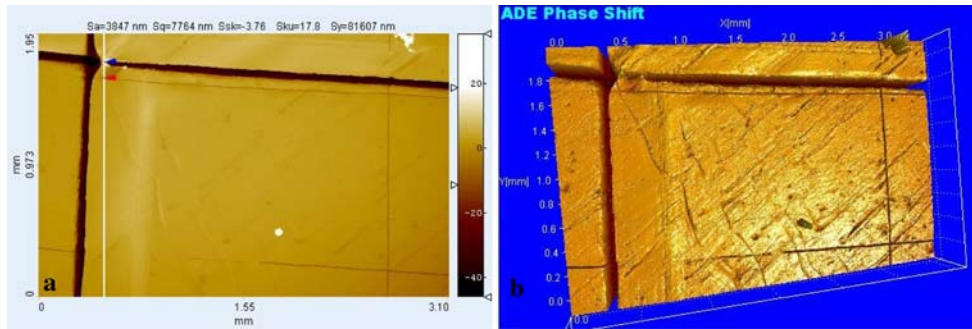


**Fig. 27** A channel network on the surface of the brass sample (a) 2D image, (b) 3D image, 20 $\times$

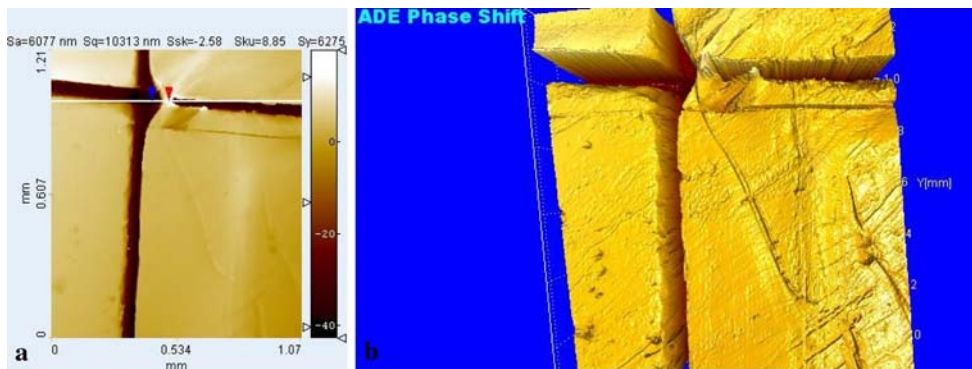


**Fig. 28** Zoomed in view of the portion of channel network shown in Fig. 27 (a) 2D image, (b) 3D image, 20 $\times$ . Notice rectangular shape of the channel

An example of profile of two adjacent channels (40 and 7  $\mu\text{m}$  wide) is shown in Fig. 25, while an example of the surface roughness measured on the bottom of the 40  $\mu\text{m}$  wide channel is depicted in Fig. 26. As it is shown by this figure, the surface roughness did not exceed 0.002  $\mu\text{m}$ .

In the course of the surface, study by the 3D profiler 3D images of sections of the micro-channels were reproduced and compliance between the die and the workpiece geometries was demonstrated for all three tested materials. The roughness, waviness, and profile analyses yielded satisfactory results.

As it is shown in Fig. 27, the brass surface contains a rectangular network of channels which is bordered by two intersecting 40  $\mu\text{m}$  wide channels (Fig. 27a). The thin lined rectangle represents 7  $\mu\text{m}$  wide channel network. Figure 27(a) is accompanied by a color bar, which depicts a range of the

depth of the formed channels. Figure 27(a) also demonstrates that a channel section shown in this figure has a depth of approximately 40  $\mu\text{m}$  along the all length of the wider channels. The 3D view of the same part the network (Fig. 27b) provides more details about the channels geometry. Particularly comparative depth of two channels is illustrated.

The zoomed views of the 40  $\mu\text{m}$  channels intersection (Fig. 28) depict fine details of channel's features. Particularly it is shown that the edges of the channels have round segments. The straight walls and the bottom of the channels are clearly shown on the 3D image.

Roughness of the channel's surfaces was analyzed by the profiler, the infinitive focus microscopy, and the 3D digital microscope. All three techniques yielded almost similar results. For example the average roughness of 1.2 mm long segment of 40  $\mu\text{m}$  wide channel was 1.6  $\mu\text{m}$  (Fig. 29a), and the average

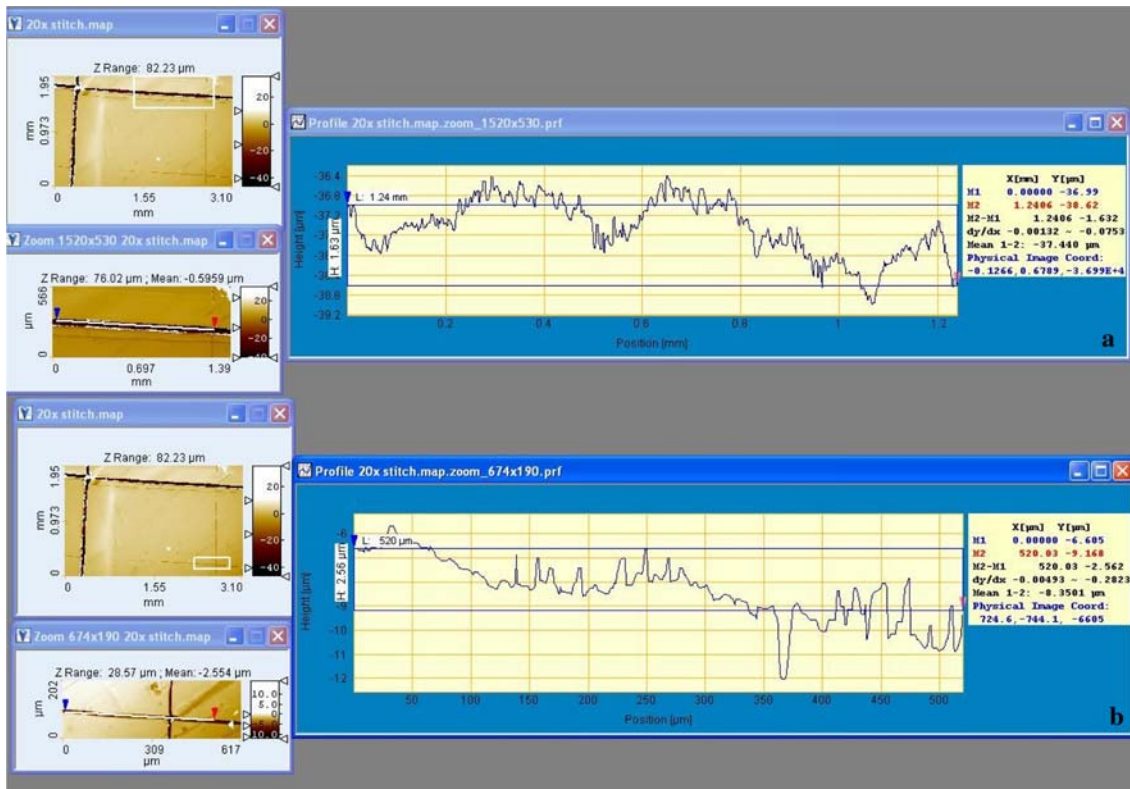


**Fig. 29** Average roughness of selected segments of channels, (a) average roughness of 1.2 mm long segment of 40  $\mu\text{m}$  wide channel was 1.6  $\mu\text{m}$  and (b) average roughness of 530  $\mu\text{m}$  long segment of 6  $\mu\text{m}$  wide channel was 2.53  $\mu\text{m}$

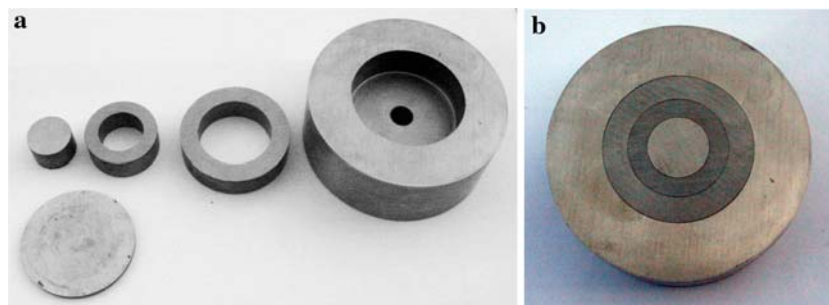


**Fig. 30** A die for ring formation: (a) disassembled and (b) assembled

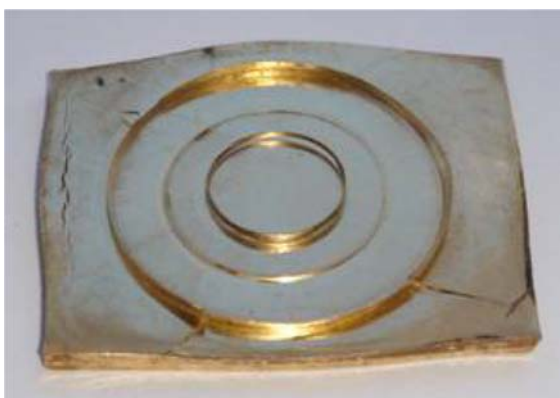


**Fig. 31** Extruded circular brass rings

roughness of 530  $\mu\text{m}$  long segment of 6  $\mu\text{m}$  wide channel (Fig. 29b) was 2.53  $\mu\text{m}$ .

#### 4.4 Micron Scale Extrusion

The objective of this study was to investigate extrusion of metals by filling a space between cylindrical and plane walls. The distance between the walls was ranged from 10 to 50  $\mu\text{m}$ , while the wall width was in order of several centimeters and the height was in order of several millimeters. Thus, process involves filling a semi-infinite micron scale gap by an impacted metal. Copper, brass, and high-ductility steel samples were used. Also, some of the samples were made from an alloy used for fabrication of Ukrainian coins. Two types of dies were designed and manufactured. The first kind of dies entails two concentric rings and a solid cylinder. The heights of the rings

and the cylinder were almost precisely equal. In the course of the die assembly, the cylinder was tightly fitted into a cylindrical ring of the precisely same height. Then, the obtained assembly was tightly fitted into another ring also having the same height (Fig. 30). The rings and the cylinder were fabricated so that in the course of the assembly micron scale gaps were formed between the cylindrical surfaces on the forefront base of the cylindrical assembly. The base of the constructed die was placed against a target. By exposing a

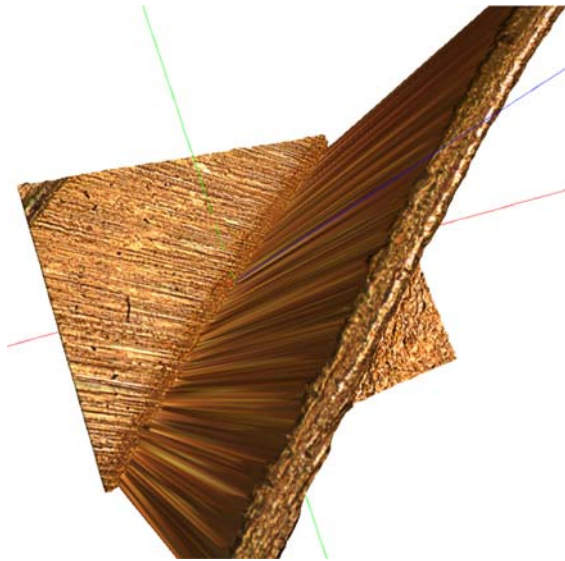


**Fig. 32** 3D image of a section of the extruded brass ring. The section is 1500  $\mu\text{m}$  high and 150  $\mu\text{m}$  thick

target to the water projectile impact, a target material was being extruded into the gap between the cylindrical surfaces creating rings (Fig. 30). While the thickness of the rings was in order of microns, the height and the diameter were in order of millimeters. Thus, micro-extrusion with comparatively high-extrusion ratio was accomplished.

Maximal extrusion ratio of 130 was achieved in a section of a cooper ring, and maximal extrusion ratio of 100 was obtained in a small section of the brass ring (Fig. 31). A segment of the extruded ring reproduced by the infinite focus microscopy is shown in Fig. 32. A selected profile of the same segment has 1500  $\mu\text{m}$  height and approximately 150  $\mu\text{m}$  thickness (Fig. 33). The extrusion ratio 10 observed in this case was substantially lower than the average one. Infinite focus microscopy was used to evaluate waviness and roughness of selected samples (Fig. 34 and 35).

As it is shown in Fig. 31-33 brass extruded at comparatively high-extrusion ratio forms rings having almost straight wall and almost plane surface. The surface topography was also adequate. According to Fig. 34, the roughness of a sample was less than 1  $\mu\text{m}$  while the waviness was approximately 10  $\mu\text{m}$  (Fig. 35). The performed profile and roughness analyses demonstrated that the extruded rings had stable micro-geometry. A segment of the extruded copper ring reproduced by the infinite focus microscopy is shown in Fig. 36. A selected transversal cross section of the segment (a foil profile) is 250  $\mu\text{m}$  high and 50  $\mu\text{m}$  thick (Fig. 37). A segment of the extruded steel ring is shown in Fig. 38 and a selected profile form the segment 400  $\mu\text{m}$  high and 90  $\mu\text{m}$  thick (Fig. 39).

The second die was used for the study of the formation of plain foils having the micron scale thickness. In order to fabricate a die, the calibration strips (15 and 25  $\mu\text{m}$  thick) were placed between 1 cm thick tool-steel slabs. This die assembly

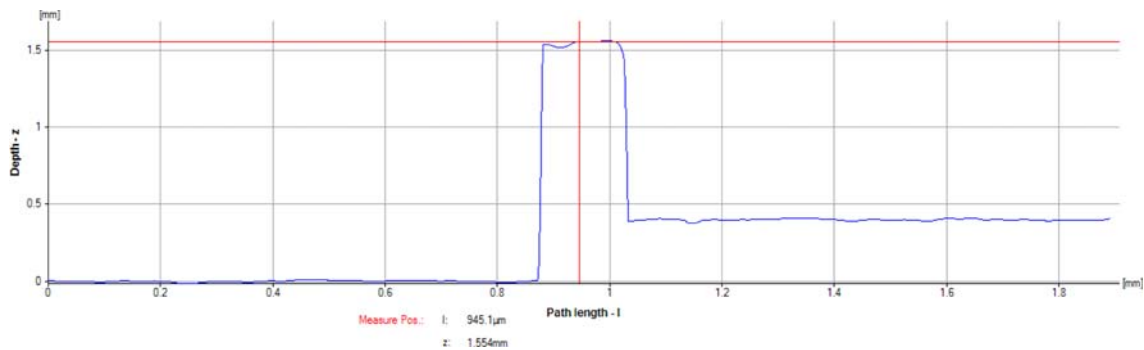


**Fig. 33** Profile of a section of the extruded brass ring. The section is 1500  $\mu\text{m}$  high and 150  $\mu\text{m}$  thick

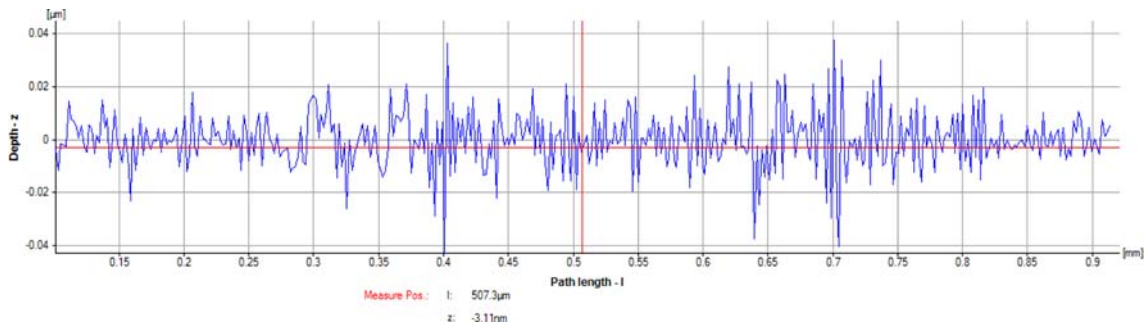


**Fig. 34** Roughness of a section of the extruded brass ring

had 6 mm deep gaps, which were 15 and 25  $\mu\text{m}$  wide. The die was fastened by a plane support. A high-strength alloy used for fabrication of the Ukrainian coins was used as a target. The target materials were extruded into the gaps (Fig. 40) and the extrusion ratio between 100 and 200 was attained in the course of these experiments.

## 5. Discussion of Results

The liquid impact based forming has unique technological advantages. For example, similarly to the explosive forming, it

requires a single die. The second die is replaced by a liquid punch. This simplifies the forming facilities and reduces its cost. A water projectile (liquid punch) could be applied to several processing operations and rapid execution of tasks would enable mass production of various parts. Contactless mode of the launcher-workpiece interaction, ability of a liquid projectile to adjust to any geometry of a die, simplicity of process control assures the flexibility of the impact based micro-forming. While the previous research (Ref 9) showed effectiveness of the application of high-speed liquid impact to conventional forming operation, this study demonstrated feasibility to extend this application to micro-forming.

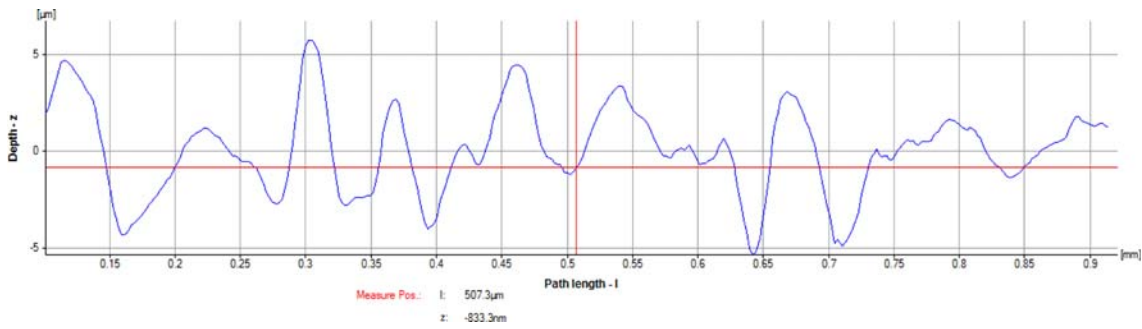


**Fig. 35** Surface waviness of brass-wall section

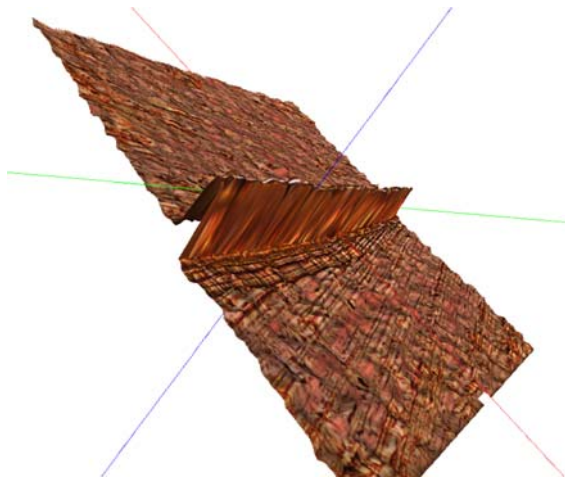


**Fig. 36** 3D image of a section of the extruded copper ring. The section is 250  $\mu\text{m}$  high and 50  $\mu\text{m}$  thick

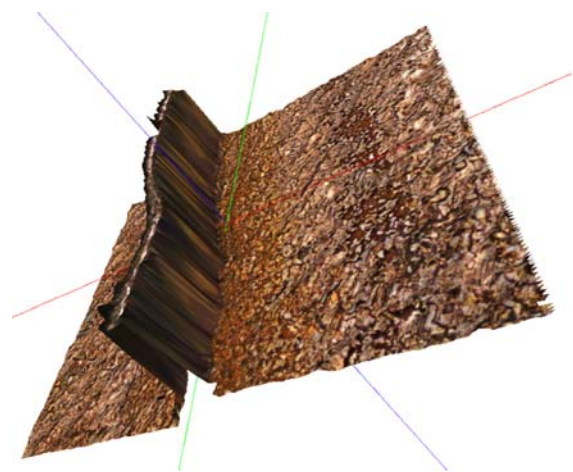


**Fig. 38** 3D image of a section of the extruded steel ring. The section is 400  $\mu\text{m}$  high and 150  $\mu\text{m}$  thick

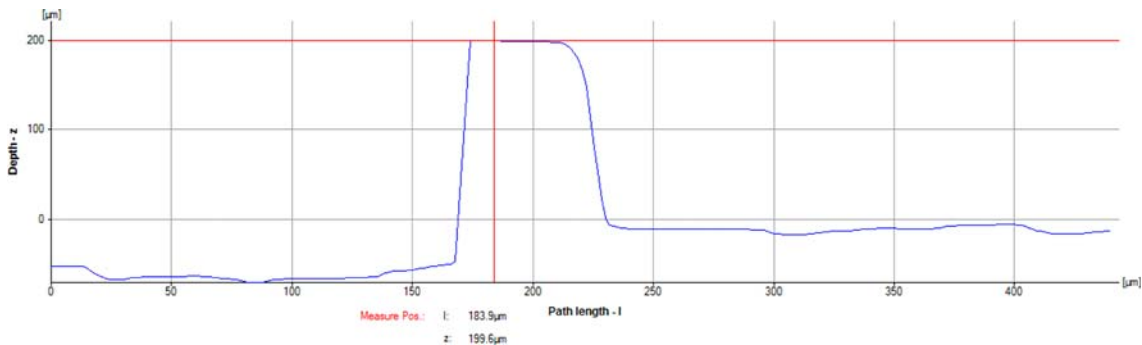


**Fig. 37** Profile of a section of the extruded copper ring. The section is 250  $\mu\text{m}$  high and 50  $\mu\text{m}$  thick

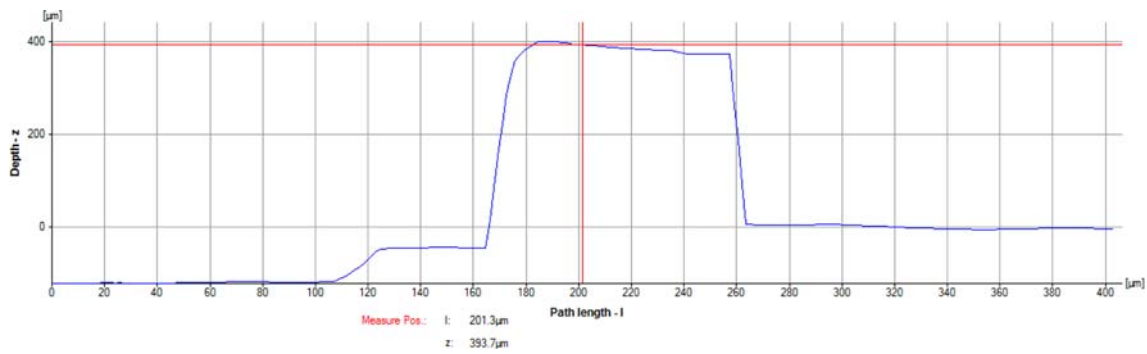


**Fig. 39** Profile of a section of the extruded steel ring. The section is 400  $\mu\text{m}$  high and 90  $\mu\text{m}$  thick

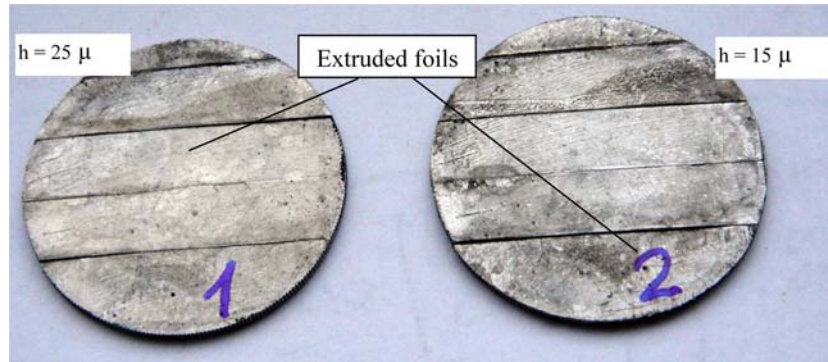


**Fig. 40** Extruded plain foils of nickel-base alloy

In the course of the performed study totally 12 testing of extrusion into closed cavities, 12 testing of extrusion into open slots, eight testing of micron scale stamping, and 11 tests of micron scale forming were carried out. All of these tests involved deformation of various metals including steel and a special alloy at an extremely high-rate determined by the speed of the water projectiles. The tests included formation of rather complex patterns such as networks of the micro-scale channels or an image of a coin. The facilities used in this study (launcher, dies, targets, and fixture) were fabricated using conventional machine shop capabilities and conventional materials. No special provisions for fastening a die, target or launcher or preventing die deformation were available. Even at these conditions only two tests did not result in completion of the selected forming operation. In the rest of experiments, the results of forming were satisfactory. The desired shapes were generated, surface topography of the targets was quite adequate, no defects or damage generated in the course of deformation were observed. Formation of shapes having a size of 6  $\mu\text{m}$  was achieved.

It is expected the development of manufacturing technology will involve mass production of the precision low-cost micron scale parts out of various engineering materials or formation of the micron scale pattern of the surfaces of regular parts. The performed experiments demonstrate feasibility of the use of high-speed projectiles for fabrication of micro-scale parts. It was shown that liquid impact driven micro-forming has a potential of becoming technology of choice for micro-parts fabrication. Indeed, the feasibility to generate micro-scale (down to 6  $\mu\text{m}$ ) parts with an adequate surface topography was demonstrated. The facilities are comparatively simple and

process productivity is determined by the firing rate of the launcher. For simplicity sake in the performed experiments, a powder was used as an energy source. It is expected that in a manufacturing environment the chemical energy of a powder will be replaced by electrical or magnetic energy. In this case, the firing rate can be as high as 1 kHz. Then it can be expected the speed of the projectiles to be increased up to 2-3 km/s and the accuracy and the strength of the dies will be significantly enhanced. This will enable us to generate more complicated and more accurate parts.

The performed experiments also indicate that there is a possibility to apply a proposed technology to micro-forming of difficult to process materials, perhaps such as glass or ceramics. Unique advantages of the liquid impact based micro-forming define the effectiveness of its application, while the performed experiments show its feasibility.

## 6. Conclusion

It was shown that forming of metals on submillimeter and micro-scale can be accomplished by high-speed water projectiles. Original concept of micro-machining process is validated. It was shown that micro-forming can be accomplished by a single water projectile impact. It was shown that it is possible to generate a single micro-object as well as an assembly of such objects, e.g., a network of micro-channels. The obtained extrusion ratio shows feasibility to fabricate micron scale foils. Since commercial low-cost metals were used in this study, it can be suggested that the use of super-plastic materials would

yield parts having grain scale dimensions. The performed experiments show that liquid projectiles have a potential of becoming a competitive micro-forming tool.

## Acknowledgments

The support of NSF (Award DMI-9900247) and CRDF (UE2-2441-DO-02 Q2) in performing of this study is acknowledged. The state of the art instrumentation techniques was provided by EXCEL Technologies, Enfield, CT 06083; Hitachi High Technologies America Inc., Gaithersburg, MD 20878; Micro Photonics Inc., Irvine, CA 92618; and ADE Phase Shift, Tuscon, AZ 85706.

## References

1. G.A. Atanov, *Hydroimpulsive Installations for Rocks Breaking*. Kiev, Vystcha shkola, 1987, in Russian
2. G. Atanov, The Impulsiv Water Jet Device: A New Machine For Breaking Rock, *International Journal of Water Jet Technology*, 1996, 1(2), p 85–91
3. W.C. Cooley and W.N. Lucke. Development and Testing of a Water Cannon for Tunneling, *Proc. of the 2nd International Symposium on Jet Cutting Technology*, Cambridge, England, Paper J3, 1974
4. B.V. Voitsekhovskiy, Jet Nozzle for Obtaining High Pulse Dynamic Pressure Heads. U.S. Patent No. 3, 343:794, 26 Sept., 1967
5. G.A. Atanov, V.I. Gubskiy, and A.N. Semko, Internal Ballistics of the Powder Hydrocannon, *Izvestia RAN, MZhG*, 6, 175–179, in Russian
6. M.D. Verson, *Impact Machining*, Verson-Allsteel Company, 1969
7. J.S. Reinhart, *Explosive Working of Metals*, Macmillan, 1963
8. A.V. Krutinin, *Explosion Deformation of Metals*. Moscow in Russian, Metallurgia, 1975
9. V. Samardzic, O. Petrenko, E.S. Geskin, G.A. Atanov, and A.N. Semko, Innovative Jet-based Material Processing Technology, *2005 WJTA American Waterjet Conference & Exhibition*, ST Louis, MO, 2005
10. V. Samardzic, Petrenko, T. Bitadze, E.S. Geskin, G.A. Atanov, A.N. Semko, A.N. Kovaliov, and O.A. Rusanova, Feasibility Study of Free Form Fabrication of the Heterogeneous Structures Using the Liquid Impact, *Proceedings of 2005 DMII NSF Grantees Conference*, Scottsdale, AZ, 2005
11. V. Samardzic, O.P. Petrenko, E.S. Geskin, G.A. Atanov, A.N. Semko, and A. Kovaliov, Innovative Jet Based Material Processing Technology, *Proceedings of Waterjet Technology Association Conference*, M. Hashish, Ed., Aug., Houston, TX; Paper 2A-2, 2005
12. K. Dohda, An Overview of Micro-Forming Research and Development in Japan, *Micro/Meso Mechanical Manufacturing Workshop*, Gifu University, Yanagido, Gifu, Japan, 2000
13. H.-J. Lee, N.-K. Lee, S.-M. Lee, G.-A. Lee, and S.-S. Kim, Development of Micro Metal Forming Manufacturing System, *Materials Science Forum*, Vols. 505–507, Trans Tech Publications, Switzerland, 2006, p 19–24
14. Friedrich-Alexander University, Micro Forming Technology, [http://www.lft.uni-erlangen.de/SEITEN/GRUPPEN/MUT/index\\_e.html](http://www.lft.uni-erlangen.de/SEITEN/GRUPPEN/MUT/index_e.html)
15. New Tool Technology by Direct Heating with Laser Radiation, *Mass Micro News Lett.*, Issue 4, Sept., 2006, <http://www.masmicro.net/Article/A243.pdf>